Electrochemical Dechlorination of Trichloroethylene by Manganese Phthalocyanine: Performance and Mechanisms

Jia Deng[1], Zheng Fang[1,*], Yitao Dai[2] and Lizhi Huang[1]

[1]*School of Civil Engineering, Wuhan University, Wuhan, Hubei, 430072, China*
[2]*Department of Applied Chemistry, University of Science and Technology of China, Hefei, 230026, China*
E-mail: zfang@whu.edu.cn
[*]*Corresponding Author*

Received 08 December 2021; Accepted 05 January 2022;
Publication 25 January 2022

Abstract

Trichloroethylene (TCE) is one of the most abundant persistent organic pollutant in subsurface environment. TCE can be reduced electrochemically, but the extremely negative applied potential limits the application of this technology. Manganese phthalocyanine (MnPc) catalyst was used for the electrochemical reductive dechlorination of TCE. The results show that MnPc can be reduced by electrons attachment at -0.21 V, -1.22 V and -1.77 V, respectively. With the decrease of applied potential from -0.3 V to -1.8 V, the transformation from TCE to dichloroethylene (DCE) efficiency increased from 19.9% to 41.8% after 5 hours of reaction. Although the electron transfer ability was enhanced with applied potential decreasing, the

Strategic Planning for Energy and the Environment, Vol. 40_4, 437–454.
doi: 10.13052/spee1048-5236.4047

intensive HER caused the electron selectivity decreased when MnPc attached more electrons. MnPc catalyze the electrochemical reduction of TCE, which has potential application on the remediation of TCE-contaminated groundwater.

Keywords: Electrochemical, dechlorination, TCE, MnPc, DFT.

1 Introduction

Trichloroethylene (TCE) is a common industrial solvents which is also abundant in environment due to the improper discharge [1]. TCE has a higher density than water and has a strong migration ability, which easily lead to the formation of TCE pollution plume in groundwater [2]. The presence of TCE brings serious hazard to human, because TCE was reported to have damages to the human nervous and reproductive system [3]. Thus, it is urgent to develop technologies for efficient removal of TCE.

Physical and chemical processes are very efficient for detoxifying TCE in groundwater [4]. TCE can be reduced electrochemically upon providing a reduction potential more negative than the dechlorination potentials of TCE [5]. However, the potential needed for direct electrochemical reduction of TCE is extremely low. Also, the low conductivity of groundwater limits the application of electrochemical technology in groundwater remediation. Precious metal such as Pd was used for electrochemical reduction of TCE, which can generate active hydrogen species with strong reduction ability at -0.6 V$\sim$$-1.2$ V to efficiently attack TCE molecule [6]. However, the high cost and the instability of metal nanoparticles have brought huge challenges to the possible practical application. Therefore, various non-precious electrocatalysts are synthesized and used in the remediation of TCE-contaminated groundwater.

Microorganisms can dechlorinate TCE to dichloroethylene (DCE) and vinyl chloride (VC) in anoxic groundwater environment [7]. The active species of these anaerobic microorganisms are metal-porphyrin structure, such as coenzyme F430, cobalamin, heme, vitamin B12, etc. [8–10]. The centre metal atom of metal-porphyrin structure as the electron transfer active site is responsible for the dechlorination activity [11, 12]. Phthalocyanine is a synthetic compound of conjugated system and the centre porphyrin structure can complex divalent metal ions. Mn-phthalocyanine (MnPc) has unique redox properties, which is directly related to electron transfer and oxygen release in plant photosynthesis [13]. In addition, MnPc as a catalyst and

photosensitizer was widely used in industrial manufacture [14, 15]. However, MnPc has been rarely used for electrocatalytic water purification.

In this work, MnPc as electrocatalysts was combined with electrochemical cathode for TCE reduction. Firstly, the electro-catalytic activity of MnPc towards TCE reduction was analysed by cyclic voltammetry. Subsequently, MnPc cathode was used for electrochemical TCE reduction at various applied potentials. Finally, the electron transfer process was characterized by electrochemical methods and analyzed though density functional theory (DFT) which reveal the catalytic mechanism.

2 Materials and Methods

2.1 Chemical Reagent

MnPc, trichloroethylene (TCE), tetrabutylammonium tetrafluoroborate (Bu_4NBF_4), N,N-dimethylformamide (DMF), anhydrous sodium sulfate (Na_2SO_4) were purchased from Sinopharm Reagent Group Chemical Reagent Co., Ltd. Dichloroethylene (DCE) including cis-dichloroethylene, trans-dichloroethylene and 1,1-dichloroethylene were purchased from Aladdin Reagent (Shanghai) Co., Ltd. Nafion D520 (5%) solution was purchased from DuPont Chemical Co., Ltd. The reagents used in the experiment were all analytical grade, and ultrapure water (conductivity $= 18.2$ MΩ.cm) was used throughout the experiment.

2.2 Electrode Preparation

MnPc (0.020 g) was added into a 1.5 mL centrifuge tube consisting of 800 μL of ultrapure water and 200 μL of Nafion solution. The mixture was sonicated for 30 minutes to obtain a catalyst ink. Subsequently, the catalyst ink was drop casted on the surface of a glassy carbon electrode (2 cm $\times$ 2 cm) with a catalyst loading of 1 mg/cm^2. Finally, the MnPc electrode was dried in the air. The procedure for the preparation of MnPc electrode is shown in Figure 1.

2.3 Electrochemical Experiments

Electrochemical experiments were performed using an electrochemical workstation (CHI600E, Shanghai Chenhua Instrument Co., Ltd.). Cyclic voltammetry data was obtained on a disc glassy carbon electrode (1.2 cm^2) with scan rate of 20 mV/s. The supporting electrolyte was 0.1 M Bu_4NBF_4 solution in DMF.

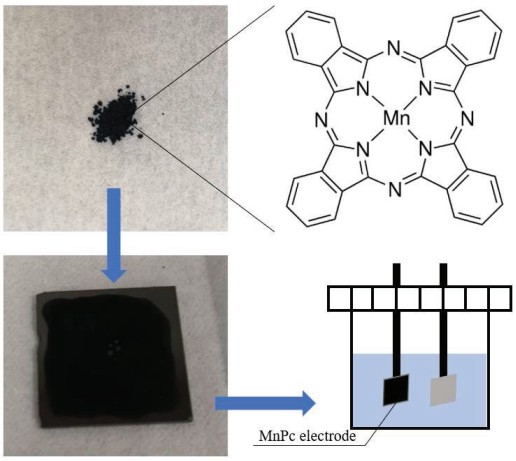

Figure 1 Procedure for the preparation of MnPc electrode.

The electrocatalytic dechlorination of TCE was carried in a 50 mL electrochemical cell. The reactor contained 30 mL reaction solution and 20 mL headspace. In order to simulate the groundwater environment, the reaction solution contained 2 mM Na_2SO_4 and 25 μM TCE, and the pH value of the reaction solution was 7.0 ± 0.2. The working electrode was the as-prepared MnPc electrode [16]. The counter electrode was a Pt plate (2 cm $\times$ 2 cm), and the reference electrode was a leak-free Ag/AgCl electrode, respectively. Electrochemical impedance spectra, Tafel curves and open circuit potentials of MnPc were determined in the same reactor using 0.5 M Na_2SO_4 aqueous solution as the supporting electrolyte.

2.4 TCE and Products Detection

The concentration of TCE and its dechlorination products were determined by a gas chromatograph (GC, GC2010, Shimadzu Corporation) equipped with an electron capture detector (ECD) and a flame ionization detector (FID). An air-tight gas syringe was used to collect a volume of 200 μL of headspace gas from the reactor for measurement.

2.5 DFT Calculation

The conformations of MnPc were optimized using Gaussian 09 software based on density functional theory (DFT) [17, 18]. DFT functional was B3LYP and a mixed basis including LANL2DZ for metallic elements and

6-31+G(d, p) for non-metallic elements were set [19, 20]. The implicit solvent-based solvation model (SMD) was used to simulate the aqueous environment [21]. The molecular orbital of MnPc was analyzed using Multiwfn software [22].

3 Result and Discussion

3.1 Cyclic Voltammetry Analysis

Previous researches reported that the reductive dechlorination potential of TCE was more negative than −2.3 V [5]. Thus, no reduction peak for TCE was observed in the absence of MnPc (Figure 2), demonstrating TCE cannot be directly reduced by glassy carbon in the potential range from 0 to −2.2 V. MnPc showed three cathodic peaks corresponding to the reduction of MnPc after attaching electrons. When TCE was added into electrolyte, the three reduction peaks were located at −0.21, −1.22 and −1.77 V, respectively. Also, the relative reduction current increased 0.06, 1.75 and 3.08 μA. This result demonstrated that the electrocatalytic activity of MnPc towards TCE reduction, and this catalytic activity was enhanced by applying more negative potentials. Therefore, controlled potential electrolysis at potentials where the cathodic peaks located was conducted.

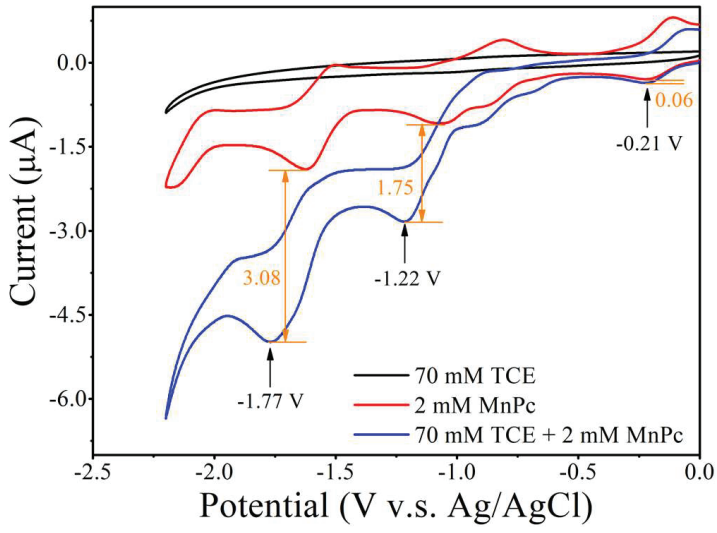

Figure 2 Cyclic voltammograms of TCE, MnPc and TCE/MnPc mixture.

3.2 Electrochemical Reduction of TCE

The cathodic peaks for TCE reduction were located at −0.21, −1.22 and −1.77 V, respectively. In order to ensure the fully electron attachment of MnPc catalyst, the applied potential was set as −0.3, −1.3 and −1.8 V. TCE decreased without applied potential and no reduction products of TCE was detected (Figure 3(a)). This result indicated MnPc without applied potential had adsorption effect on TCE [23, 24]. When the applied potential was −0.3 V, 19.9% TCE was transformed to DCE after 5 hours of reaction (Figure 3(b)). The reduction efficiency of TCE reached to 26.2% at a potential of −1.3 V (Figure 3(c)). At −1.8 V, 41.8% TCE was reduced to DCE (Figure 3(d)). When negative potential was applied, the carbon balance during the electrolysis remained stable, indicating the transformation from TCE to DCE on MnPc electrode was fast. TCE contained three electronic rich Cl atoms. Electron-attached MnPc could repel TCE molecules via electrostatic repulsion, lead to the weakened adsorption when negative potentials were applied on MnPc electrode. With the applied potential become more negative,

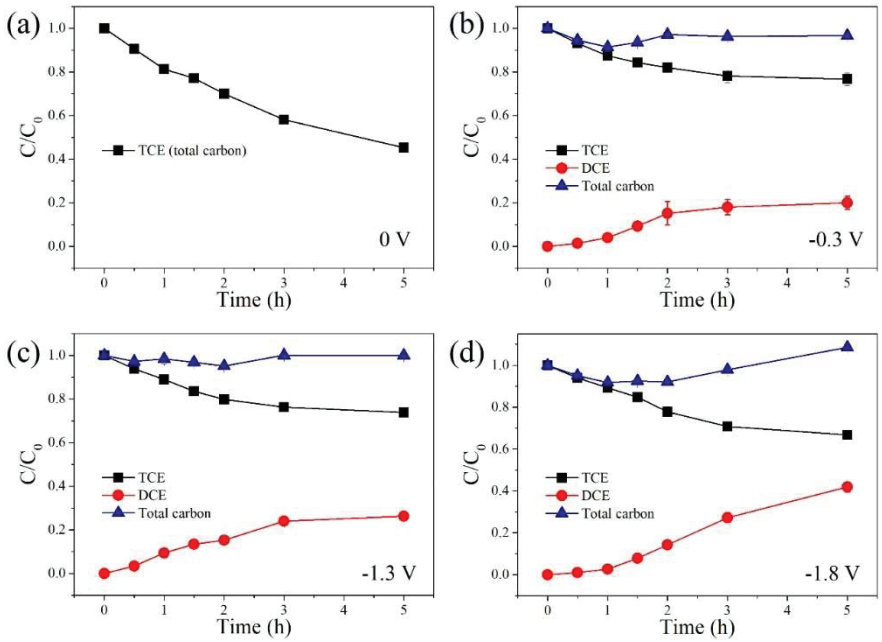

Figure 3 Electrochemical reduction of TCE by MnPc electrode at (a) 0 V, (b) −0.3 V and (c) −1.3 V and (d) −1.8 V vs. Ag/AgCl.

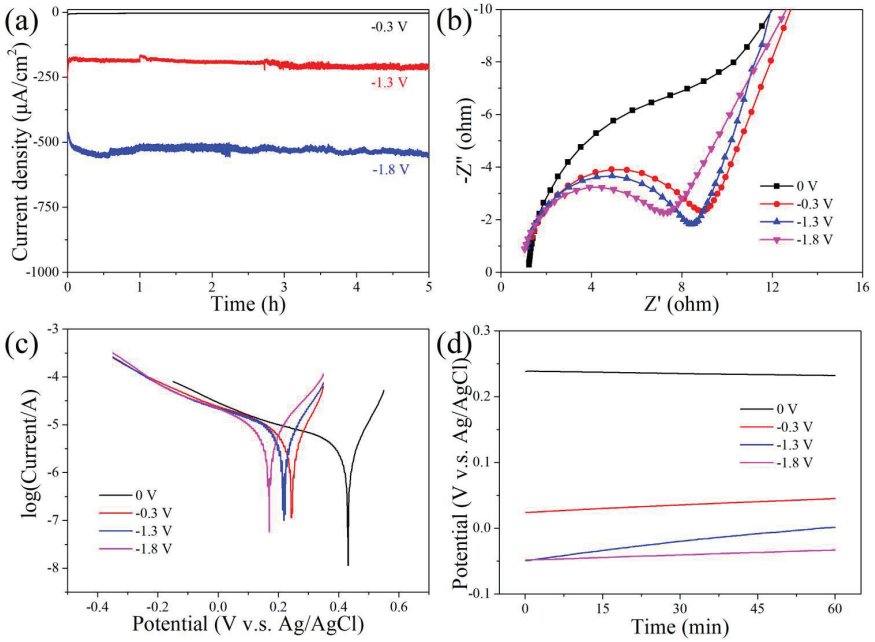

Figure 4 Electrochemical characterization of MnPc after applying different potentials. (a) i-t curves, (b) Electrochemical impedance spectra (c) Tafel curves and (d) open circuit potentials of MnPc.

the reductive catalytic performance of MnPc increased which is in line with the CV analysis.

As shown in Figure 4(a), the current density of MnPc at −0.3, −1.3 and −1.8 V which were −5, −200 and −520 μA/cm^2. The stable current density proved the continuous reduction of TCE on MnPc electrode. In addition, the current density increased significantly with potential decreasing, indicating the electron transfer efficiency may be higher at more negative potential. The increase of MnPc's catalytic performance was mainly attributed to the improved electron transfer efficiency. Thus, the electrochemical analysis of MnPc after electrolysis at different potentials was carried out. The arc radius in the EIS of MnPc became smaller with more negative potentials (Figure 4(b)), proving that electron attachment on MnPc was conducive to interfacial electron transfer [25]. The corrosion currents of MnPc (Table 1) can be obtained by fitting the Tafel curves (Figure 4(c)). The corrosion currents of MnPc increased if the potential become more negative, proving that the electron transfer process was enhanced after electrons attachment to

Table 1 Corrosion current of MnPc after applying different potentials

Potential	Corrosion Current (A)
0 V	2.72×10^{-6}
−0.3 V	3.71×10^{-6}
−1.3 V	6.20×10^{-6}
−1.8 V	7.62×10^{-6}

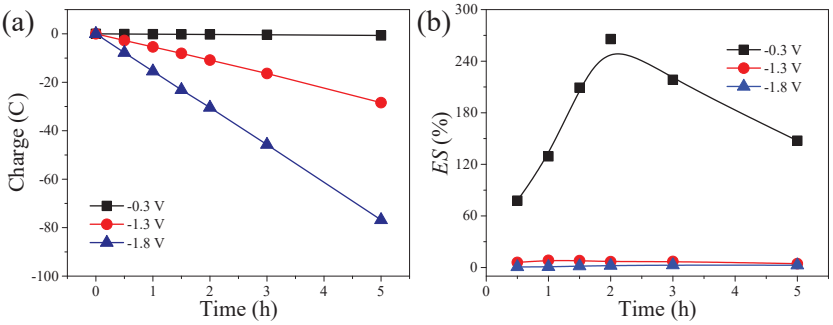

Figure 5 (a) The input charge corresponding to different applied potentials. (b) The electron selectivity during electrochemical reduction process.

MnPc. The open-circuit potentials of MnPc was more negative as the applied potential decreases (Figure 4(d)), which further confirmed that the electron transfer was enhanced when MnPc was attached with electrons [26].

Notably, the high electron transfer efficiency may result in the intensive hydrogen evolution reaction (HER), thereby causing the energy consumption. Therefore, the electron selectivity (*ES*) should be investigated which represents the proportion of electrons contributing on the dechlorination of TCE. The breakage of one C–Cl bond needs two electrons [27]. The electrons contributing on the dechlorination of TCE can be calculated according to TCE removal and DCE generation. The input charge corresponding to different applied potentials can be obtained in Figure 5(a). Hence, *ES* was calculated according to the ratio of the charge required for TCE-to-DCE conversion and the total input charge (Equation (1)). As shown as Figure 5(b), the *ES* value at −0.3 V was obviously higher than −1.3 V and −1.8 V. Although MnPc showed a high TCE reduction efficiency at −1.3 V and −1.8 V, most of the input charge was used for the HER and the reduction of MnPc. The value of ES was higher than 100% at −0.3 V demonstrating that the electrons of MnPc may be transfer to TCE.

$$ES = \text{e(dechlorination)/e(total input)} \tag{1}$$

3.3 DFT Analysis

In order to investigate the property of electron transfer on MnPc, the conformations of MnPc and electrons-attached MnPc were optimized by DFT. MnPc consist of the Mn center and the Pc structure. When electrons were attached on MnPc, the mulliken charge of Mn and Pc was changed (Table 2). Figure 6 showed the mulliken charge on Pc decreased faster than Mn, indicating the attached electrons was more intensively distributed on the Pc structure. Notably, the atomic charge will be re-distributed on MnPc when electron attached to MnPc. The spin density of MnPc attaching electrons also changed. The spin of MnPc was quartet indicating three unpaired electrons existed in MnPc [28]. With the electron attachment to MnPc, the unpaired electrons gradually decreased. Thus, the conformations of MnPc + e and MnPc + 2e had two and one unpaired electrons, respectively. When three electrons attached to MnPc, the conformation became closed shell state. As shown in Figure 7, the spin area increased when one electron attaching to MnPc conformation. The spin density was concentrated at the central Mn atom of MnPc and MnPc + e conformation. However, the spin area decreased when two electrons attaching to MnPc and the spin disappeared on MnPc + 3e conformation. Electronic spin reflects the electronic activity. MnPc at −0.3 V had the highest electron selectivity for TCE reduction, which may be attributed to the large spin area of MnPc + e conformation.

Due to the electrons attachment, the highest occupied molecular orbital (HOMO) and lowest unoccupied molecular orbital (LUMO) of MnPc

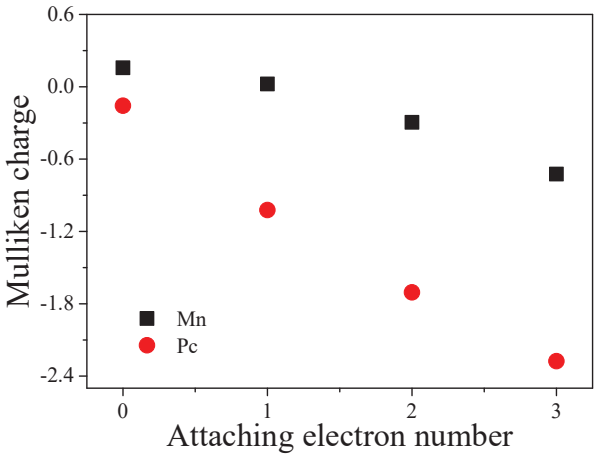

Figure 6 The change of mulliken charge on Mn and Pc when electrons are attached to MnPc.

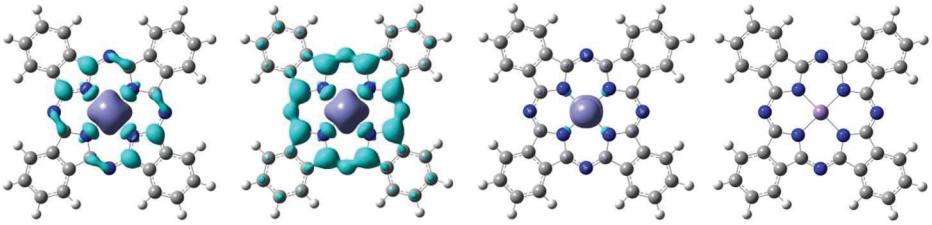

Figure 7 Spin density of MnPc and electrons-attached MnPc.

Table 2 The mulliken charge on Mn and Pc when electrons were attached to MnPc

	Mulliken Charge of Mn	Mulliken Charge of Pc	Total Charge
MnPc	0.157	−0.157	0
MnPc + e	0.023	−1.023	−1
MnPc + 2e	−0.295	−1.705	−2
MnPc + 3e	−0.724	−2.276	−3

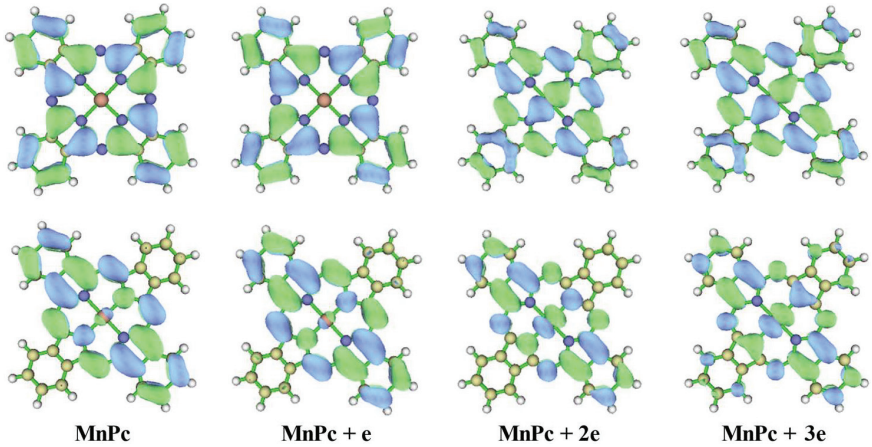

Figure 8 HOMO (up image) and LUMO (low image) of the MnPc conformation and the electrons-attached MnPc conformations.

changed gradually (Figure 8). On the conformations of MnPc and MnPc + e, HOMO orbitals concentrated towards the structure of Pc and the central Mn atom had the LUMO orbitals. As the catalytic site, Mn atom had the better catalytic activity when one electron attaching to MnPc due to the unbalance HOMO-LUMO. HOMO-LUMO orbitals was all concentrated the central Mn atom when two and three electrons attaching to MnPc. Although

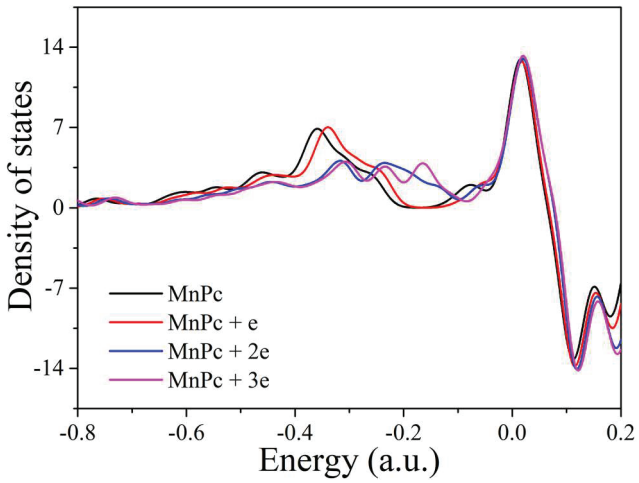

Figure 9 The calculated PDOS plots of Mn site on MnPc and electrons-attached MnPc.

the conductivity of MnPc electrode increased with electrons attachment, the catalytic efficiency of MnPc electrode decreased with electrons attachment.

We also calculated the partial density of states (PDOS) of Mn site on MnPc and electrons-attached MnPc. As shown in Figure 9, shows that the central Mn site of MnPc and MnPc + e had a higher PDOS at −0.4∼–0.3 a.u than MnPc + 2e and MnPc + 3e. In the other energy range, these four conformations had the close PDOS. This result indicated the Mn site of MnPc + e conformation had a better electrocatalytic activity than MnPc + 2e and MnPc + 3e conformations [11]. In summary, MnPc without applied potential had the adsorption effect to TCE which was attributed to the electrostatic effect. Mn site of MnPc is in divalent state which can lose electron to become Mn^{3+} or higher valence. When one electron attached to MnPc at −0.3 V, Mn site of MnPc had the highest catalytic activity causing the dechlorination of TCE. With applied potential decreasing, the electron catalytic ability of the central Mn atom becomes weaker but the total electron input increased. Although the dechloriantion efficiency of TCE was higher at −1.8 V and −1.3 V, the electron selectivity was highest at −0.3 V.

4 Conclusion

MnPc can adsorb TCE and show electrocatalytic activity towards TCE reduction. With the applied potential becoming more negative, the reduction

efficiency of TCE increased due to the enhanced electron transfer ability. However, the atomic charge will be re-distributed on MnPc when electron attached to MnPc. The conformation of MnPc + e had the largest spin area and Mn site of MnPc + e conformation had a better electrocatalytic activity than MnPc + 2e and MnPc + 3e conformations. Thus, the electron selectivity was highest at −0.3 V. This work provides a novel application on the remediation of TCE-contaminated groundwater.

Acknowledgement

This work was financially supported by the National Natural Science Foundation of China (Grant Nos. 41807188 and 51978537), the Fundamental Research Funds for the Central Universities (2042021kf0201), and Start-up Fund for Distinguished Scholars, Wuhan University (1403-413100041, 1403-600460022). The numerical calculations in this paper have been done on the supercomputing system in the Supercomputing Center of University of Science and Technology of China.

References

[1] J. Ai, W. Yin, H.C.B. Hansen, Fast dechlorination of chlorinated ethylenes by green rust in the presence of bone char. *Environmental Science & Technology Letter*, 6 (2019) 191–196.

[2] A.J. Rabideau, J.M. Blayden, C. Ganguly, Field performance of air-sparging system for removing TCE from groundwater. *Environmental Science & Technology*, 33 (1999) 157–162.

[3] K.Z. Guyton, K.A. Hogan, C.S. Scott, G.S. Cooper, A.S. Bale, L. Kopylev, S. Barone, S.L. Makris, B. Glenn, R.P. Subramaniam, Human health effects of tetrachloroethylene: key findings and scientific issues. *Environmental Health Perspectives* 122 (2014) 325–334.

[4] H. Liu, T.A. Bruton, F.M. Doyle, D.L. Sedlak, In situ chemical oxidation of contaminated groundwater by persulfate: Decomposition by Fe(III)- and Mn(IV)-containing oxides and aquifer materials. *Environmental Science & Technology*, 48 (2014) 10330–10336.

[5] C. Lei, F. Liang, J. Li, W. Chen, B. Huang, Electrochemical reductive dechlorination of chlorinated volatile organic compounds (Cl-VOCs): Effects of molecular structure on the dehalogenation reactivity and mechanisms. *Chemical Engineering Journal*, 358 (2019) 1054–1064.

[6] G. Jiang, M. Lan, Z. Zhang, X. Lv, Z. Lou, X. Xu, F. Dong, S. Zhang, Identification of active hydrogen species on palladium nanoparticles for an enhanced electrocatalytic hydrodechlorination of 2,4-dichlorophenol in water. *Environmental Science & Technology*, 51 (2017) 7599–7605.

[7] P.K. Sharma, P.L. Mccarty, Isolation and Characterization of a Facultatively Aerobic Bacterium That Reductively Dehalogenates Tetrachloroethene to cis-1,2-Dichloroethene. *Applied and Environmental Microbiology*, 62 (1996) 761–765.

[8] G.M. KleèKa, S.J. Gonsior, Reductive dechlorination of chlorinated methanes and ethanes by reduced iron (II) porphyrins. *Chemosphere*, 13 (1984) 391–402.

[9] U.E. Krone, K. Laufer, R.K. Thauer, H. Hogenkamp, Coenzyme F430 as a possible catalyst for the reductive dehalogenation of chlorinated C1 hydrocarbons in methanogenic bacteria. *Biochemistry* 28 (1989) 10061–10065.

[10] L. Ukrainczyk, M. Chibwe, T.J. Pinnavaia, S.A. Boyd, Reductive dechlorination of carbon tetrachloride in water catalyzed by mineral-supported biomimetic cobalt macrocycles. *Environmental Science & Technology*, 29 (1995) 439–445.

[11] G. Gan, X. Li, L. Wang, S. Fan, J. Mu, P. Wang, G. Chen, Active sites in single-atom Fe-N_x-C nanosheets for selective electrochemical dechlorination of 1,2-dichloroethane to ethylene. *ACS Nano*, 14 (2020) 9929–9937.

[12] Y. Xu, Z. Yao, Z. Mao, M. Shi, B. Liu, Single-Ni-atom catalyzes aqueous phase electrochemical reductive dechlorination reaction. *Applied Catalysis B: Environmental*, 277 (2020) 119057.

[13] L.J. Boucher, Manganese porphyrin complexes. *Coordination Chemistry Reviews*, 7 (1972) 289–329.

[14] A. Arshak, S. Zleetni, K. Arshak, β-radiation sensor using optical and electrical properties of manganese phthalocyanine (MnPc) thick film. *Sensors*, 2 (2002) 174–184.

[15] E. Urbain, F. Ibrahim, M. Studniarek, F.N. Nyakam, L. Joly, J. Arabski, F. Scheurer, F. Bertran, P. Le Fevre, G. Garreau, Cu metal/Mn phthalocyanine organic spinterfaces atop Co with high spin polarization at room temperature. *Advanced Functional Materials*, (2017).

[16] J. Deng, X.-M. Hu, E. Gao, F. Wu, W. Yin, L.-Z. Huang, D.D. Dionysiou, Electrochemical reductive remediation of trichloroethylene contaminated groundwater using biomimetic iron-nitrogen-doped carbon. *Journal of Hazardous Materials*, 419 (2021) 126458.

[17] M.J. Frisch, G.W. Trucks, H.B. Schlegel, G.E. Scuseria, J.R.C. M. A. Robb, G. Scalmani, V. Barone, G. A. Petersson, H. Nakatsuji, X. Li, M. Caricato, A. Marenich, J. Bloino, B. G. Janesko, R. Gomperts, B. Mennucci, H. P. Hratchian, J. V. Ortiz, A. F. Izmaylov, J. L. Sonnenberg, D. Williams-Young, F. Ding, F. Lipparini, F. Egidi, J. Goings, B. Peng, A. Petrone, T. Henderson, D. Ranasinghe, V. G. Zakrzewski, J. Gao, N. Rega, G. Zheng, W. Liang, M. Hada, M. Ehara, K. Toyota, R. Fukuda, J. Hasegawa, M. Ishida, T. Nakajima, Y. Honda, O. Kitao, H. Nakai, T. Vreven, K. Throssell, J. A. Montgomery, Jr., J. E. Peralta, F. Ogliaro, M. Bearpark, J. J. Heyd, E. Brothers, K. N. Kudin, V. N. Staroverov, T. Keith, R. Kobayashi, J. Normand, K. Raghavachari, A. Rendell, J. C. Burant, S. S. Iyengar, J. Tomasi, M. Cossi, J. M. Millam, M. Klene, C. Adamo, R. Cammi, J. W. Ochterski, R. L. Martin, K. Morokuma, O. Farkas, J. B. Foresman, and D. J. Fox,, GAUSSIAN 09. Gaussian, Inc., Wallingford, CT, p. 2009., in.

[18] A.D. Becke, Density-functional thermochemistry. III. The role of exact exchange. *The Journal of Chemical Physics*, 98 (1998) 5648–5652.

[19] P. Jeffrey, H. Willard, R. Wadt, Ab initio effective core potentials for molecular calculations. Potentials for the transition metal atoms Sc to Hg. *The Journal of Chemical Physics*, 82 (1985) 270–270.

[20] T. Chen, J. Ma, Q. Zhang, Z. Xie, Y. Zeng, Degradation of propranolol by UV-activated persulfate oxidation: Reaction kinetics, mechanisms, reactive sites, transformation pathways and Gaussian calculation. *Science of the Total Environment*, 690 (2019) 878–890.

[21] A.V. Marenich, C.J. Cramer, D.G. Truhlar, Universal solvation model based on solute electron density and on a continuum model of the solvent defined by the bulk dielectric constant and atomic surface tensions. *The Journal of Physical Chemistry B*, 113 (2009) 6378–6396.

[22] T. Lu, F. Chen, Multiwfn: A multifunctional wavefunction analyzer. *Journal of Computational Chemistry*, 33 (2012) 580–592.

[23] S.K. Eshkalak, M. Khatibzadeh, E. Kowsari, A. Chinnappan, S. Ramakrishna, A novel surface modification of copper (II) phthalocyanine with ionic liquids as electronic ink. *Dyes and Pigments*, (2018) S0143720817320454.

[24] J.D. Wright, Gas adsorption on phthalocyanines and its effects on electrical properties. *Progress in Surface Science*, 31 (1989) 1–60.

[25] J. Zhang, Q. Ji, H. Lan, G. Zhang, H. Liu, J. Qu, Synchronous reduction–oxidation process for efficient removal of trichloroacetic acid: H*

initiates dechlorination and ·OH is responsible for removal efficiency. *Environmental Science & Technology*, 53 (2019) 14586–14594.

[26] Y. Hu, X. Peng, Z. Ai, F. Jia, L. Zhang, Liquid Nitrogen Activation of Zero-Valent Iron and Its Enhanced Cr(VI) Removal Performance. *Environmental Science & Technology*, 53 (2019) 8333–8341.

[27] J. Deng, X. Zhan, F. Wu, S. Gao, L.-Z. Huang, Fast dechlorination of trichloroethylene by a bimetallic $Fe(OH)_2$/Ni composite. *Separation and Purification Technology*, 278 (2022) 119597.

[28] T. Kataoka, Y. Sakamoto, Y. Yamazaki, V.R. Singh, A. Fujimori, Y. Takeda, T. Ohkochi, S.-I. Fujimori, T. Okane, Y. Saitoh, H. Yamagami, A. Tanaka, Electronic configuration of Mn ions in the π-d molecular ferromagnet β-Mn phthalocyanine studied by soft X-ray magnetic circular dichroism. *Solid State Communications*, 152 (2012) 806–809.

Biographies

Jia Deng is an Eng.D. student at the school of civil engineering Wuhan University since autumn 2019. He received his bachelor of engineering degree from Shihezi University in 2016. He received his master of engineering degree from Hefei University of Technology in 2019. His research interests include reductive dehalogenation of halogenated pollutants, iron-based environmental materials and advanced oxidation process.
Email: Jagger@whu.edu.cn.

Zheng Fang, corresponding author, received his master of engineering degree from Xi'an University of Architecture and Technology and obtained a Ph.D. from Wuhan University. He is currently a doctoral supervisor of Wuhan University, a member of the National Steering Committee of Water Supply and Drainage Science and Engineering of Higher Education Institutions, director of Hubei Urban Comprehensive Disaster Prevention and Fire Rescue Engineering Technology Research Center. He is a member of the Building Water Supply and Drainage Committee of the Architectural Society, a member of the Fire Safety Engineering Sub-Committee of the National Standardization Committee and an expert member of the China Water Supply and Drainage Pipeline Association. His main research directions are: building water supply and drainage and fire protection, municipal pipeline network and sponge city, municipal engineering disaster prevention and mitigation. Email: zfang@whu.edu.cn.

Yitao Dai, received his master of science degree from Dalian University of Technology and obtained a Ph.D. from Aarhus University. He was a

postdoctoral researcher at Max-Planck-Institute in Germany and was awarded the title of "Humboldt Scholar". He joined University of Science and Technology of China Suzhou Institute for Advanced Research in August 2021. His research direction is heterogeneous catalysis. Email: yitaodai@ustc.edu.cn.

Lizhi Huang, received his master of engineering from Huazhong University of Science and Technology and obtained a Ph.D. from University of Copenhagen. He is currently a doctoral supervisor of Wuhan University, a high-level talent in Hubei Province, a member of the Youth Committee of China Water Association, and a member of the International Water Association. His research interests are iron environmental chemistry and water pollution control. Email: huanglizhi1984@foxmail.com.